

Particle concentration influences inertial focusing in Multiorifice Flow Fractionation microfluidic devices

Xavier Casadevall i Solvas, Andrew J deMello

Chemistry and applied biosciences, Swiss Federal Institute of Technology in Zurich

 **Correspondence**

xavier.casadevall@chem.ethz.ch

 **Disciplines**

Microfluidics

 **Keywords**

Multiorifice Flow Fractionation

Inertial Microfluidics

 **Type of Observation**

Standalone

 **Type of Link**

Standard Data

 **Submitted** May 3, 2016

 **Published** Oct 26, 2016



Triple Blind Peer Review

The handling editor, the reviewers, and the authors are all blinded during the review process.



Full Open Access

Supported by the Velux Foundation, the University of Zurich, and the EPFL School of Life Sciences.



Creative Commons 4.0

This observation is distributed under the terms of the Creative Commons Attribution 4.0 International License.

Abstract

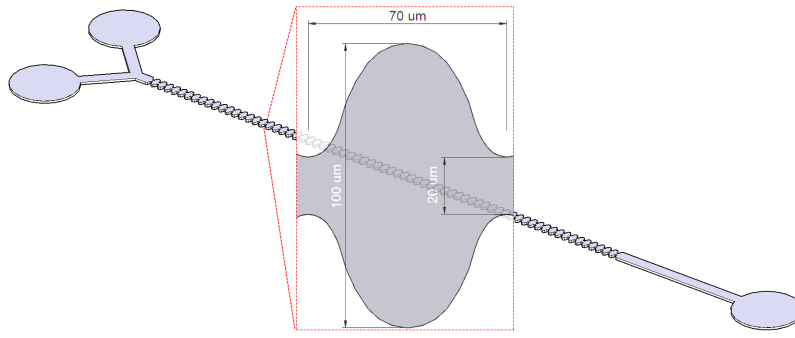
Multiorifice Flow Fractionation (MOFF) devices have been used for the separation of microparticles and cells according to their size and the degree of inertia (i.e. Re number). Herein an additional parameter, particle concentration, is reported to affect the performance of MOFF when the remaining conditions are unchanged. Particularly, at low concentrations focusing occurs efficiently at the center of these devices, while at higher concentrations particles tend to accumulate near the channel walls. This indicates that particle-particle interactions are a key component in the performances of these devices.

Introduction

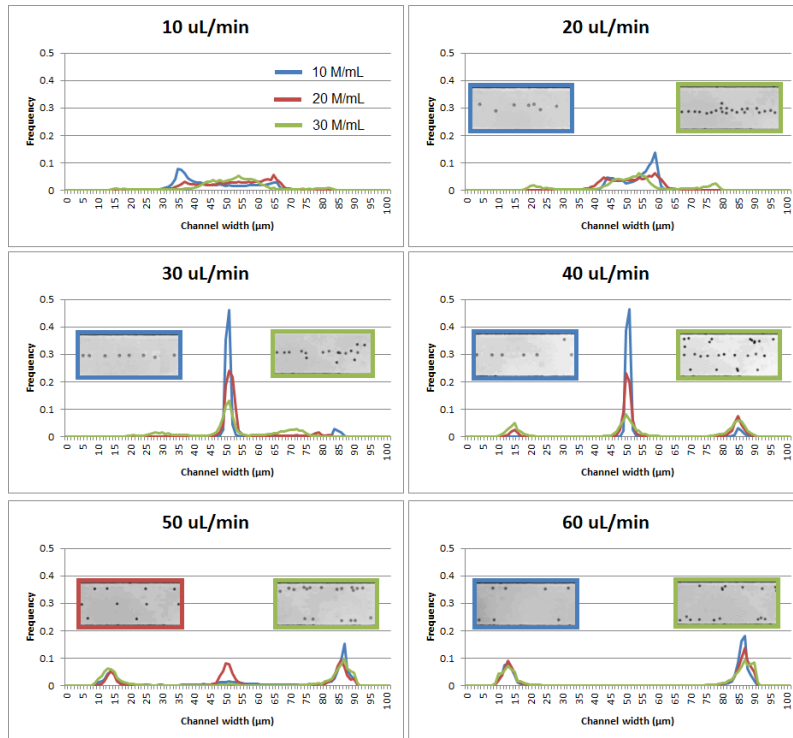
Particles in suspension driven through MOFF devices experience inertial forces that equilibrate them at specific focusing positions [1]. This process has been shown to depend on two main parameters: Re number and particle size [2]. At low Re, particles are randomly distributed through the width of the device, while at medium and high Re, particles focus laterally (in two extremely opposed focusing lines) and at the center of the device, respectively. The transition between lateral and central focusing occurs earlier for larger particles. Therefore, when operated at adequate Re regimes, larger particles (which focus at the center of the device) can be separated from smaller particles (which focus laterally). A mechanism behind this separation has been suggested [2], but, as we have shown with this observation, this picture is still incomplete: when operating smaller MOFF devices under similar Re regimes but at different particle concentrations, both the focusing efficiency and modes (either central or lateral) are affected. This suggests that the focusing mechanism is a more complex phenomenon, which is also influenced by orifice size and particle-particle interactions.

Objective

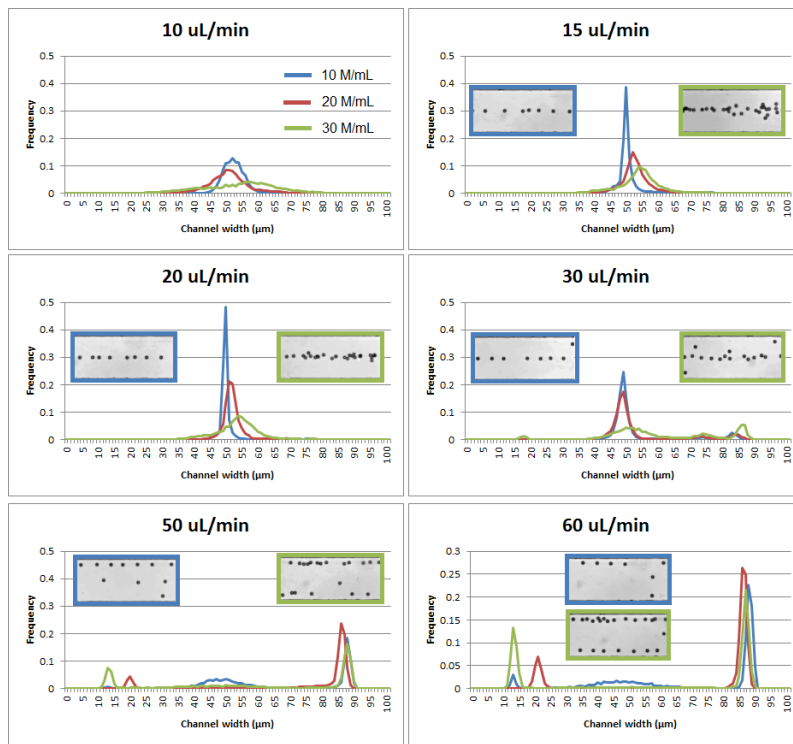
The objective is to demonstrate the effect of particle concentration on the focusing performance of small MOFF devices.



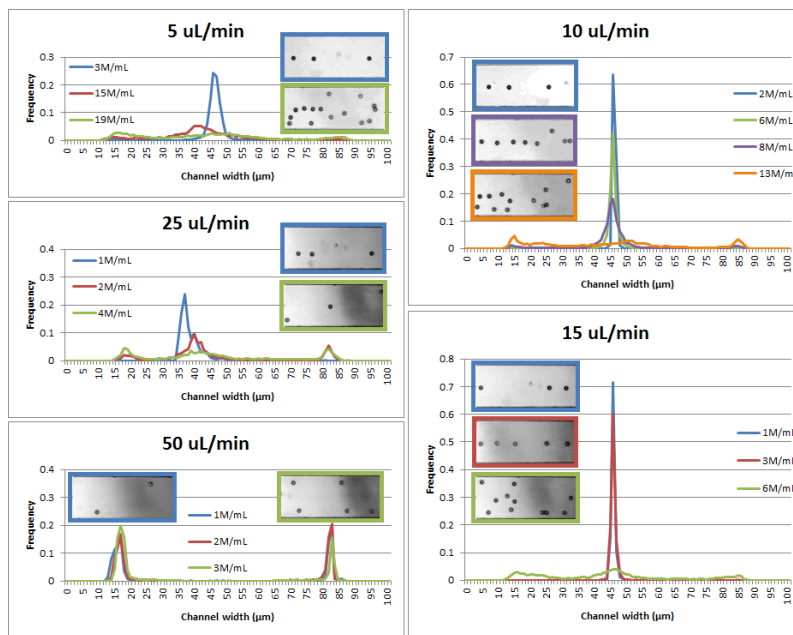
a



b



c



d

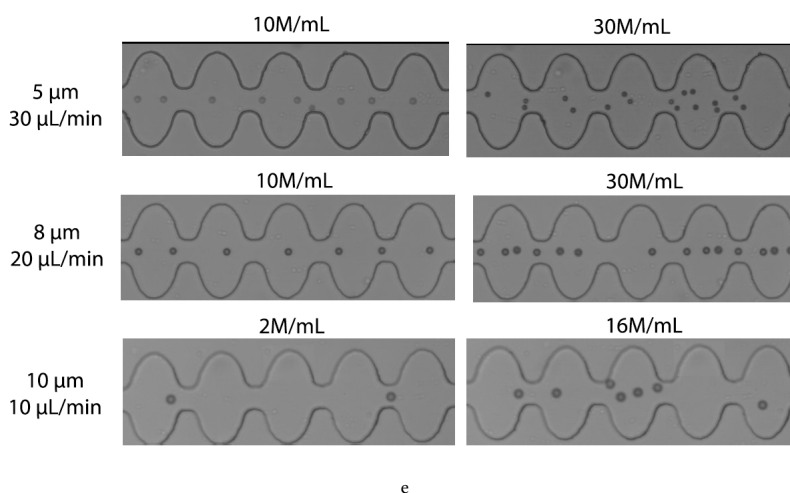


Figure Legend

Figure 1.

(A) Design and dimensions of the MOFF device (of 20 μm in height). Two inlets were used for the infusion of the particle-laden solutions and for the infusion of buffer to fine tune the concentration of particles on-chip. Particle images were acquired in the 100 μm wide section at the end of the device.

(B) Focusing histograms of 5 μm particles at different flow rates for several concentrations each. At sufficiently inertial regimes (flow rates > 20 $\mu\text{L}/\text{min}$) particles begin to focus at the center of the device (histogram peaks appear at the middle of the width). The peaks are always taller and narrower for conditions of lower particle concentrations. The transition between central to lateral focusing begins to occur earlier for higher particle concentrations. At 40 $\mu\text{L}/\text{min}$, there are three similar peaks for the highest concentration, while at the lowest concentration there is mostly a single peak, with a smaller one beginning to appear at one lateral of the channel. At 50 $\mu\text{L}/\text{min}$, the central peak disappears from the higher concentration conditions, while three peaks (central and lateral) are clearly visible for the lowest concentration conditions. At the final flow rate of 60 $\mu\text{L}/\text{min}$ lateral focusing is predominant for all concentration conditions.

(C) Focusing histograms of 8 μm particles at different flow rates for several concentrations each. At sufficiently inertial regimes (flow rates > 10 $\mu\text{L}/\text{min}$) particles begin to focus at the center of the device. The peaks are always taller and narrower for conditions of lower particle concentrations. Central to lateral focusing again occurs earlier for higher particle concentrations, beginning at 30 $\mu\text{L}/\text{min}$: three peaks appear for the highest concentration, while at the lowest concentration there is mostly a single peak (with a smaller one beginning to appear at on lateral of the channel). At 50 $\mu\text{L}/\text{min}$, the central peak disappears from the higher concentration conditions, while at the lowest concentration conditions a central peak is still observed (though quiet broad). Even at 60 $\mu\text{L}/\text{min}$, where lateral focusing is predominant for all concentration conditions, there is still a (broad) peak for the lowest concentration conditions.

(D) Focusing histograms of 10 μm particles at different flow rates for several concentrations each. At sufficiently inertial regimes (flow rates > 5 $\mu\text{L}/\text{min}$) particles begin to focus at the center of the device. The peaks are always taller and narrower at lower particle concentrations. Central to lateral focusing again occurs earlier for higher particle concentrations, beginning at only 10 $\mu\text{L}/\text{min}$: two lateral peaks appear for the highest concentration, while at the lowest concentrations there is only a tall and narrow single peak in the middle of the channel. At 25 $\mu\text{L}/\text{min}$ only at the lowest concentration a single peak is maintained at the center (though short and broad). At 50 $\mu\text{L}/\text{min}$ lateral focusing occurs in all concentrations.

(E) Orifice section for different particle diameters at different concentrations (under same flow regimes). It can clearly be seen that at higher concentrations particles become crowded near the orifices.

Device fabrication

MOFF devices were manufactured in PDMS (Sylgard® 184, Dow Corning, Biesterfeld Spezialchemie GmbH, Hamburg, Germany) using standard soft lithographic methods. PDMS was casted on silicon wafers patterned with 20 μm thick SU-8 photoresist (Micro Resist Technology GmbH, Germany) shaped with the opposite motifs of the MOFF micro-channel device. Once cured, the structured PDMS layer was subsequently bonded to a glass slide by treatment with oxygen plasma.

Particle suspension preparation

Polystyrene particles (Sigma-Aldrich Chemie GmbH, Switzerland) of 5, 8 and 10 μm were suspended at a concentration of 35 M/mL in a density-matched aqueous solution prepared by dissolving NaCl in filtered, deionized water until the final desired density of $\rho = 1.05 \text{ g/mL}$ was achieved. 0.1% Tween-20 was also added to prevent particle aggregation.

Experimental setup and imaging

Suspensions of particles and buffer were infused through the device with the use of two syringe pumps (neMESYS, Cetoni, Germany). Images were acquired with a Phantom MIRO 310 high-speed camera (Vision Research Ltd., UK) and processed with ImageJ.

Data analysis

The precise concentration of particles in the device was calculated by analyzing the amount of particles in each frame and dividing it by the volume of the section of the device under observation. Particle position histograms along the width of the MOFF device were constructed by analyzing the high-speed camera images using the DMV Matlab routine for droplet/particle analysis [3]. Each analyzed data set consisted of $N > 1000$ particles (typically > 10000 for particle concentrations $> 5 \text{ M}$). **Results & Dis-**

cussion

Several experiments were carried out using the MOFF device shown in figure 1A (with a height of 20 μm). Since the purpose of the experiments was to demonstrate the effects of particle concentration in focusing performance, the dimensions of the device were kept constant in all experiments. Density-matched aqueous suspensions of polystyrene particles (with diameters of 5, 8 and 10 μm) were used in the experiments. The two inlets of the device were used to pump in two different solutions: the particle-laden suspension and buffer (used to dilute and fine tune the particle's concentration on-chip). This allowed the rapid exploration of a diversity of concentrations and Re regimes, by simply changing the flow rate ratio between the two solutions while maintaining the total flow rate. The particles were imaged in a 100 μm -wide section immediately downstream from the last orifice.

The first relevant observation we present is in terms of the focusing mode observed in our experiments. At low and intermediate Re, the tendency of the particles is to focus at the center of the channel, while at larger Re the focus tends to happen laterally (at the two opposite extremes of the channel width). This is in direct contrast with previous reports of MOFF devices, where lateral focusing occurs at lower/medium Re and central focusing at higher Re [2]. Although it is beyond the scope of this work to discuss it here, we presume that this discrepancy possibly arises from the ratio between the particle diameter and the orifice size, which is much higher in our device than in other MOFF devices characterized before.

We next show that particle concentration also has an effect on the focusing regime. This is illustrated in figures 1B, C and D, for particle diameters of 5, 8 and 10 μm , respectively, at different concentrations and flow rates. As it can be seen in all cases, the higher the concentration of particles is, the earlier (*i.e.* at lower Re) the transition toward lateral focusing begins to occur (with frequency peaks in the histograms appearing at the extremes of the chart). This effect of concentration on the transition from mid-channel to lateral focusing is best illustrated for 10 μm particles flowing at a total flow rate of 10 $\mu\text{L}/\text{min}$ (Fig. 1D). At the lowest particle concentration, a very tall and narrow peak at the center of the device is obtained, while the highest concentration two small peaks begin to arise at the edges of the device.

A final relevant phenomenon that was observed is that the focusing performance of the MOFF device in the central focusing mode is very good (*i.e.* very narrow and tall frequency peaks at the middle of the channel) when the concentrations are lowest (ideally

under 2 M/mL). This is apparent in all cases studied, but is more clearly seen, again, for the case of 10 μm particles at 10 $\mu\text{L}/\text{min}$. The higher the concentration is, the shorter and broader the frequency peaks at the mid-channel, until at the highest concentration that peak disappears and only two small peaks can be seen at the laterals of the channel. Particularly, when compared to the 8 or 5 μm particles cases, the mid-channel focusing performance with 10 μm particles at low concentrations is much better: a frequency peak over 0.7 is achieved with 10 μm particles, while the highest peaks observed for 5 and 8 μm particles are always under 0.5. This is likely because the lowest concentrations studied in 5 and 8 μm cases were substantially higher than the lowest concentrations of 10 μm particles (which were, indeed very low), and the optimum conditions for mid-channel focusing were never reached in these cases.

Figure 1E shows how at higher particle concentrations particles begin to crowd in the orifice sections. Together with the previous observations, this indicates that in conditions where particles cannot interact with each other (given the scarcity of neighbors) the focusing at the mid-channel is preferred at low and medium Re regimes. At the same regimes, though, when particle-particle interactions are common place, lateral focusing is induced. Therefore, a key mechanism that governs both the mode of focusing and its quality is likely to arise from particle-particle interactions, which seem to disrupt the performance of the mid-plane focusing mechanism while increasing the likelihood of particles to focus laterally instead.

Conclusions

Particle concentration in MOFF devices clearly affects both the mode of focusing (*i.e.* central or lateral) and the performance of focusing (*i.e.* height and narrowness of peaks in the frequency distribution of particles across the device's width) at low and intermediate Re. At these regimes, for low particle concentrations focusing occurs at the center of the channel with a very narrow frequency distribution of particles. At higher particle concentrations, this peak dramatically shrinks (and widens) and focusing at the edges of the channel is observed. These results point toward particle-particle interactions playing a key role in the mechanism of inertial focusing phenomena in MOFF devices.

We hypothesize that several mechanisms are in place that drive different modes of particle focusing, some of them being more prominent at intermediate and low Re (leading to mid-plane focusing) and others at higher Re regimes (leading to lateral focusing). The crowding of the orifices with several particles might help reduce the efficacy of the mid-plane focusing mechanism and would allow particles to be "displaced" to the lateral positions, where they are then stabilized by the second mechanism.

Additional Information

Methods

Device fabrication

MOFF devices were manufactured in PDMS (Sylgard[®] 184, Dow Corning, Biesterfeld Spezialchemie GmbH, Hamburg, Germany) using standard soft lithographic methods. PDMS was casted on silicon wafers patterned with 20 μm thick SU-8 photoresist (Micro Resist Technology GmbH, Germany) shaped with the opposite motifs of the MOFF micro-channel device. Once cured, the structured PDMS layer was subsequently bonded to a glass slide by treatment with oxygen plasma.

Particle suspension preparation

Polystyrene particles (Sigma-Aldrich Chemie GmbH, Switzerland) of 5, 8 and 10 μm were suspended at a concentration of 35 M/mL in a density-matched aqueous solution prepared by dissolving NaCl in filtered, deionized water until the final desired density of $\rho = 1.05 \text{ g/mL}$ was achieved. 0.1% Tween-20 was also added to prevent particle aggregation.

Experimental setup and imaging

Suspensions of particles and buffer were infused through the device with the use of two syringe pumps (neMESYS, Cetoni, Germany). Images were acquired with a Phantom MIRO 310 high-speed camera (Vision Research Ltd., UK) and processed with ImageJ.

Data analysis

The precise concentration of particles in the device was calculated by analyzing the amount of particles in each frame and dividing it by the volume of the section of the device under observation. Particle position histograms along the width of the MOFF device were constructed by analyzing the high-speed camera images using the DMV Matlab routine for droplet/particle analysis [3]. Each analyzed data set consisted of N >1000 particles (typically >10000 for particle concentrations >5 M).

Supplementary Material

Please see <https://sciencematters.io/articles/201606000007>.

Ethics Statement

Citations

- [1] Jae-Sung Park, Suk-Heung Song, and Hyo-Il Jung and. "Continuous focusing of microparticles using inertial lift force and vorticity via multi-orifice microfluidic channels". In: *Lab on a Chip* 9.7 (2009), pp. 939–948. DOI: 10.1039/b813952k. URL: <http://dx.doi.org/10.1039/b813952k>.
- [2] Jae-Sung Park and Hyo-Il Jung and. "Multiorifice Flow Fractionation: Continuous Size-Based Separation of Microspheres Using a Series of Contraction/Expansion Microchannels". In: *Analytical Chemistry* 81.20 (Oct. 2009), pp. 8280–8288. DOI: 10.1021/ac9005765. URL: <http://dx.doi.org/10.1021/ac9005765>.
- [3] Amar S. Basu and. "Droplet morphometry and velocimetry (DMV): a video processing software for time-resolved, label-free tracking of droplet parameters". In: *Lab on a Chip* 13.10 (2013), pp. 1892–1901. DOI: 10.1039/c31c50074h. URL: <http://dx.doi.org/10.1039/c31c50074h>.